Zeolitic Imidazolite Framework Derived Bifunctional N, P-codoped Hollow Carbon Sphere Electrocatalysts Decorated with Co_2P/Fe for Rechargeable Zn-air Batteries

Songlin Zhao[a], Maolin Liu[a], Chengcai Wang[a], Luhang Cai[a], Wei Sun[b,*], and Zhihong Zhu[a,*]

[a]Institute of Nano-science and Nano-technology, College of Physical Science and Technology, Central China Normal University, Wuhan 430079, P.R. China.

[b]Key Laboratory of Laser Technology and Optoelectronic Functional Materials of Hainan Province, College of Chemistry and Chemical Engineering, Hainan Normal University, Haikou 571158, PR China

*Corresponding author

Email: zhzhu@mail.ccnu.edu.cn (Z. Zhu), sunwei@hainnu.edu.cn (W. Sun)

1. Experimental Section

1.1. Characterizations

The morphology of the materials was received by applying scanning electron microscopy (SEM, JEOL JSM-7900F). Internal structure and corresponding element mapping were obtained by using transmission electron microscope (TEM, Talos F200x). The crystalline phase of various materials was collected by an X-ray diffractometer (XRD, PANalytical X'Pert PRO). The Raman spectrum was recorded on a Raman Spectrometer (HORIBA France SAS). The X-ray photoelectron spectroscopy (XPS) was carried out on an ESCALAB 250Xi spectrometer. The N_2

adsorption/desorption isotherms were acquired by BET measurement on a JW-BK200C.

1.2. Electrochemical Test

Electrochemical tests were measured on a CHI760e electrochemical workstation with a standard three-electrode system for ORR and OER experiments. Pt plate was used as the counter electrode and the reference electrode was the Ag/AgCl electrode with saturated 3 M KCl solutions. The inner diameter of 5.0 mm of the rotating disk electrode or the diameter of 5.61 mm rotating ring-disk electrode served as the working electrode to load the catalysts. The Co_2P/Fe/NP-HCSs suspension was obtained by dispersing 5 mg catalyst in 980 μL aqueous isopropanol (700 μL deionized and 280 μL isopropanol), followed by adding 20 ul 5 wt% Nafion solution and ultrasonic treatment for 3 h to obtain a uniform suspension ink. Then, 10 ul homogeneous sample ink was drop-cast onto a glossy working electrode and further dried at 48 ℃ before measurements. the catalyst activities were evaluated by the linear sweep voltammetry (LSV) method with a scan speed of 5 mV s^{-1} at RDE. The durability performance of catalysts was examined by i-t chronoamperometry at a proper potential. Electrochemical impedance text was carried out under 1.57 V vs. RHE in 0.1 M KOH.

To further explore the reaction mechanism of ORR, Electron transfer number, and HO_2^- yield was received by RRDE tests. The calculation formula was as follows:

$$n = 4\frac{I_d}{I_d + I_r/N} \quad (1)$$

$$H_2O_2(\%) = 200\frac{I_r/N}{I_d + I_r/N} \quad (2)$$

where I_d and I_r represent the disk electrode current and the ring electrode current, respectively, and the value of N is 0.37 which is the Pt ring collection efficiency.

1.3. Zn–Air Battery Test

First, 20 mg Co_2P/Fe/NP–HCSs was uniformly dispersed in 2 ml ethanol, 60 μL Nafion solution, and 20 μL polytetrafluoroethylene (PTFE) emulsion, sonicated for 6 h to receive a homogeneous ink. The PTFE and active carbon were stirred into a doughlike paste in the volume ratio of 7:3 by adding a fitting amount of ethanol. Then the paste was uniformly coated on a nickel foam and the ink further was sprayed on the above nickel foam, which finally dried at 50 ℃ for 3 h to obtain the eventual air electrode. The as-prepared catalyst load based on the practical substrate mass was 1mg cm^{-2}. For comparison, the commercial Pt/C and RuO_2 mixture with a loading of 1 mg cm^{-2} was applied to prepare the corresponding air electrode. The mixed solution containing 6 M KOH solution and 0.2 M $Zn(AC)_2$ aqueous solution was used as the alkaline electrolyte. A polished Zn foil was applied as the anode. The further flexible ZABs were prepared as follow:2.0 g PVA and 1.0 g KOH powder mixture was dissolved in 20.0 ml deionized water and stirring 3 h at 90 ℃. Subsequently, yellow PVA/KOH hydrogel was transferred to a laboratory plastic ware and put in the fridge for freezing to obtain a PVA membrane. Finally, the above-prepared catalyst electrode and polished Zinc foil were pressed with a thin PVA membrane to assemble flexible ZABs. All the battery tests were based on a CHI760e workstation.

2. Supplementary Figures and Table

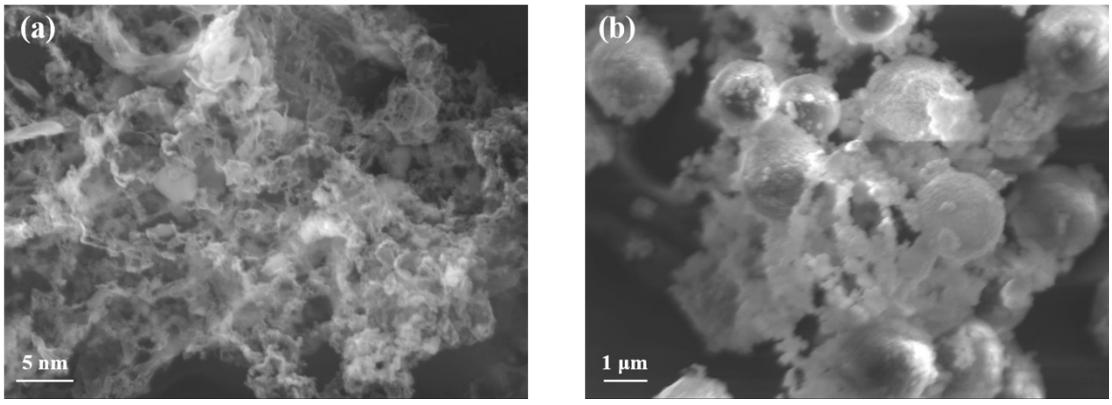

Fig. S1. (a-b) SEM images of ferrocene and PS@ZnCo–ZIF/PA/ferrocene.

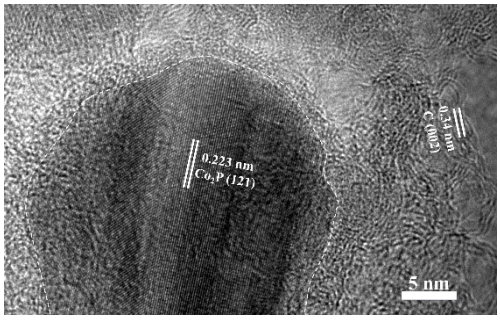

Fig. S2. TEM image of Co_2P/Fe/NP–HCSs.

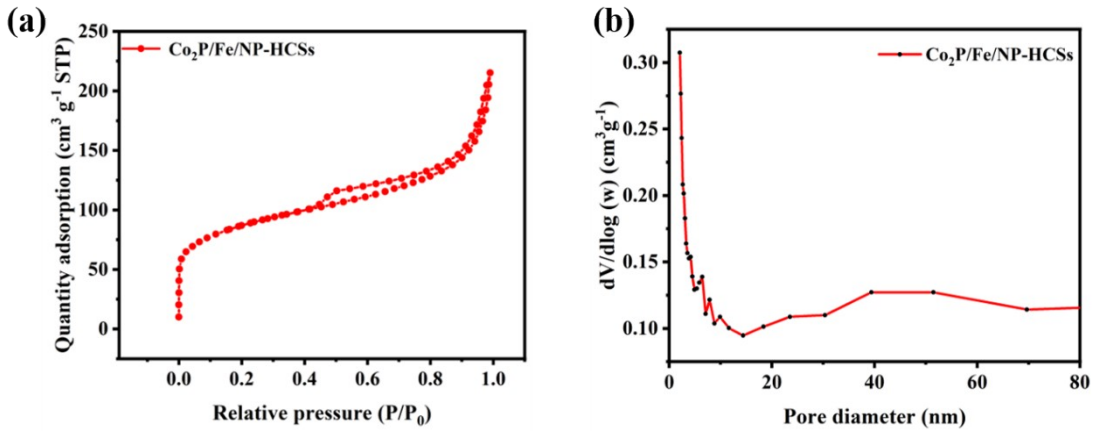

Fig. S3. (a) N_2 adsorption-desorption isotherm and (b) the corresponding pore size distribution of Co_2P/Fe/NP–HCSs.

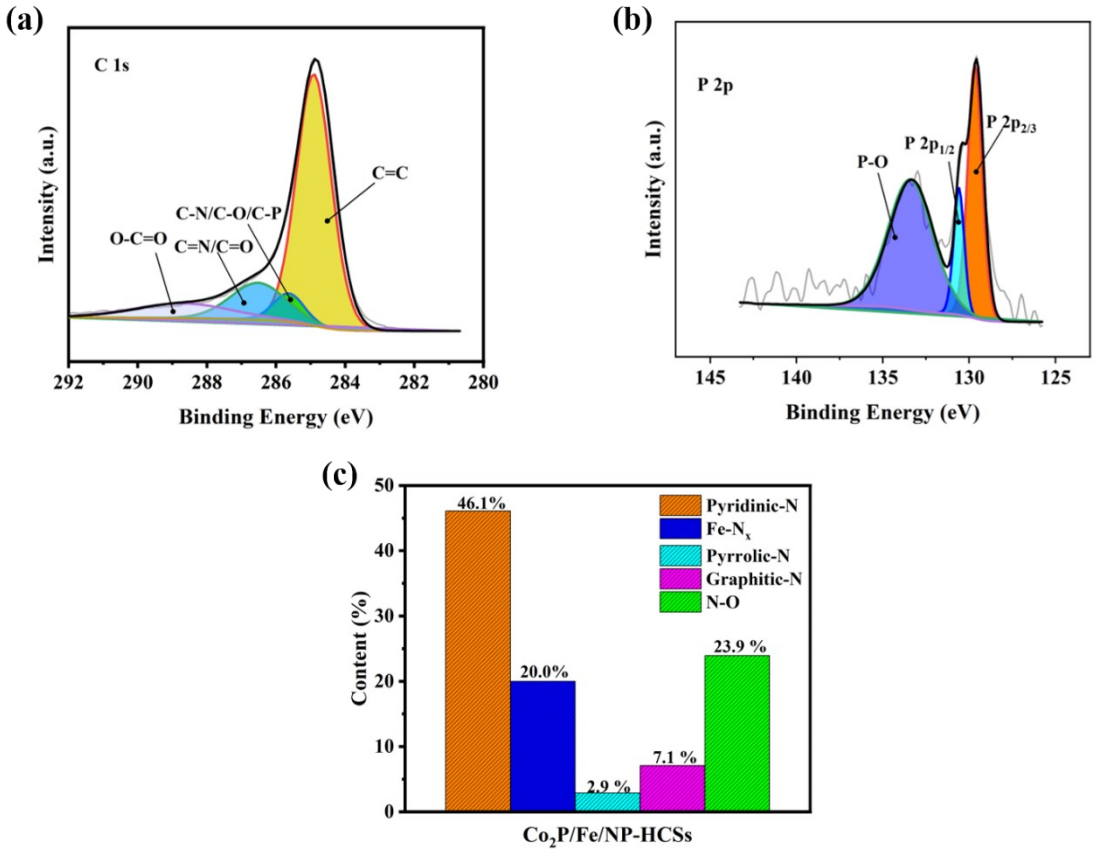

Fig. S4. High-resolution XPS spectra of (a) C 1s and (b) P 2p for Co_2P/Fe/NP–HCSs.

(c) Proportion of various nitrogen types in Co_2P/Fe/NP–HCSs.

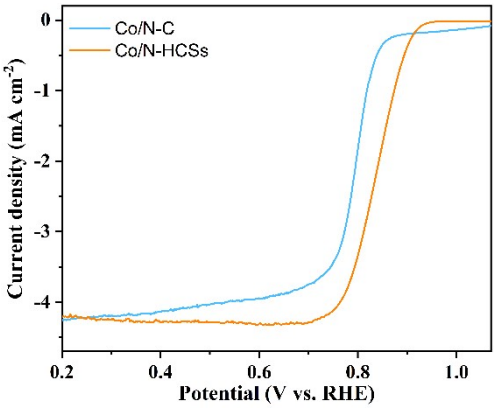

Fig. S5. LSV curves of Co/N-C and Co_2P/Fe/NP–HCSs for ORR.

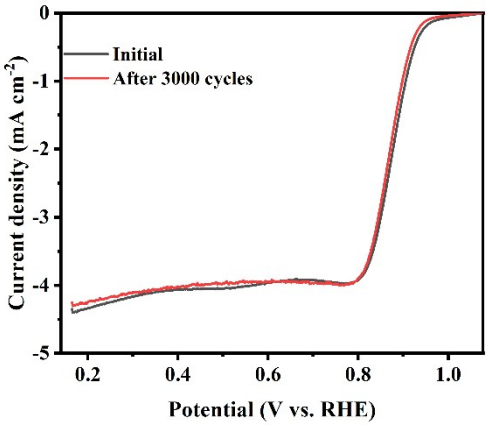

Fig. S6. LSV curves of Co_2P/Fe/NP–HCSs before and after 3000 cycles.

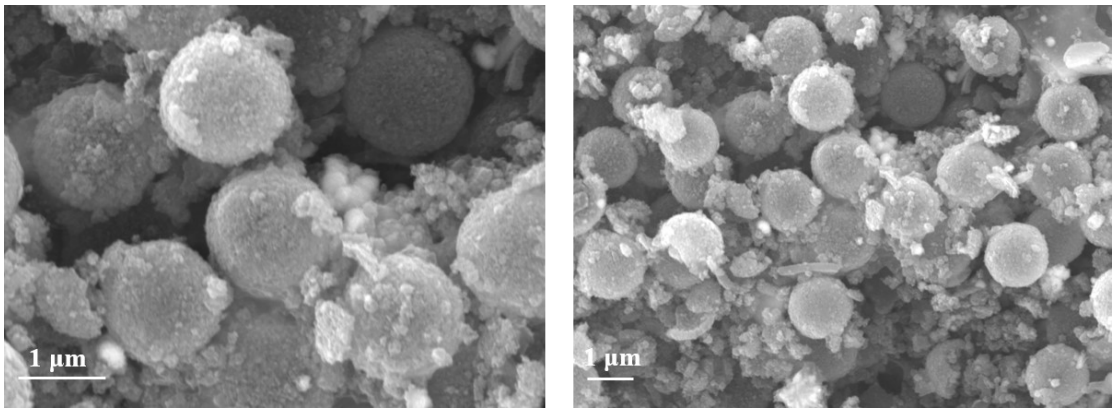

Fig. S7. SEM images of Co_2P/Fe/NP–HCSs after 3000 cycles in 0.1 M KOH.

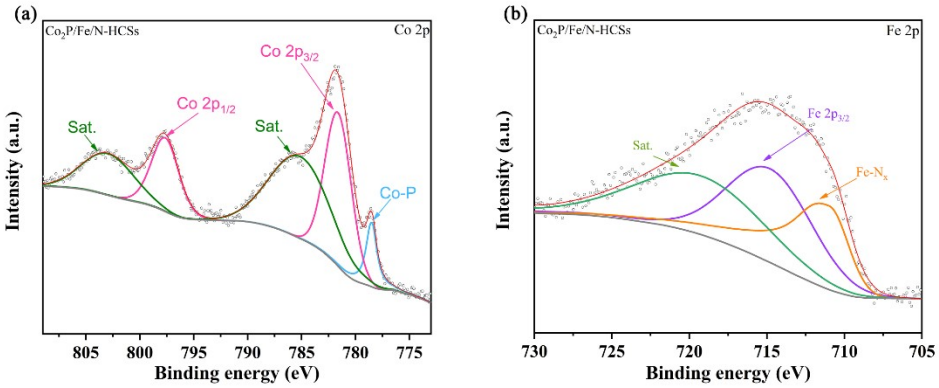

Fig. S8. XPS spectra after the ORR test.

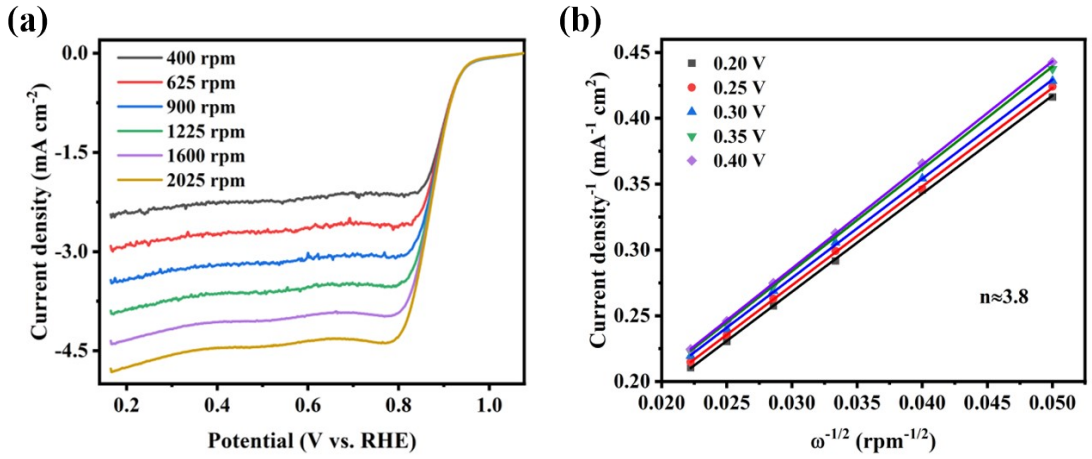

Fig. S9. (a) LSV curves in increasing rotating rates and (b) corresponding K-L plots of Co_2P/Fe/NP–HCSs.

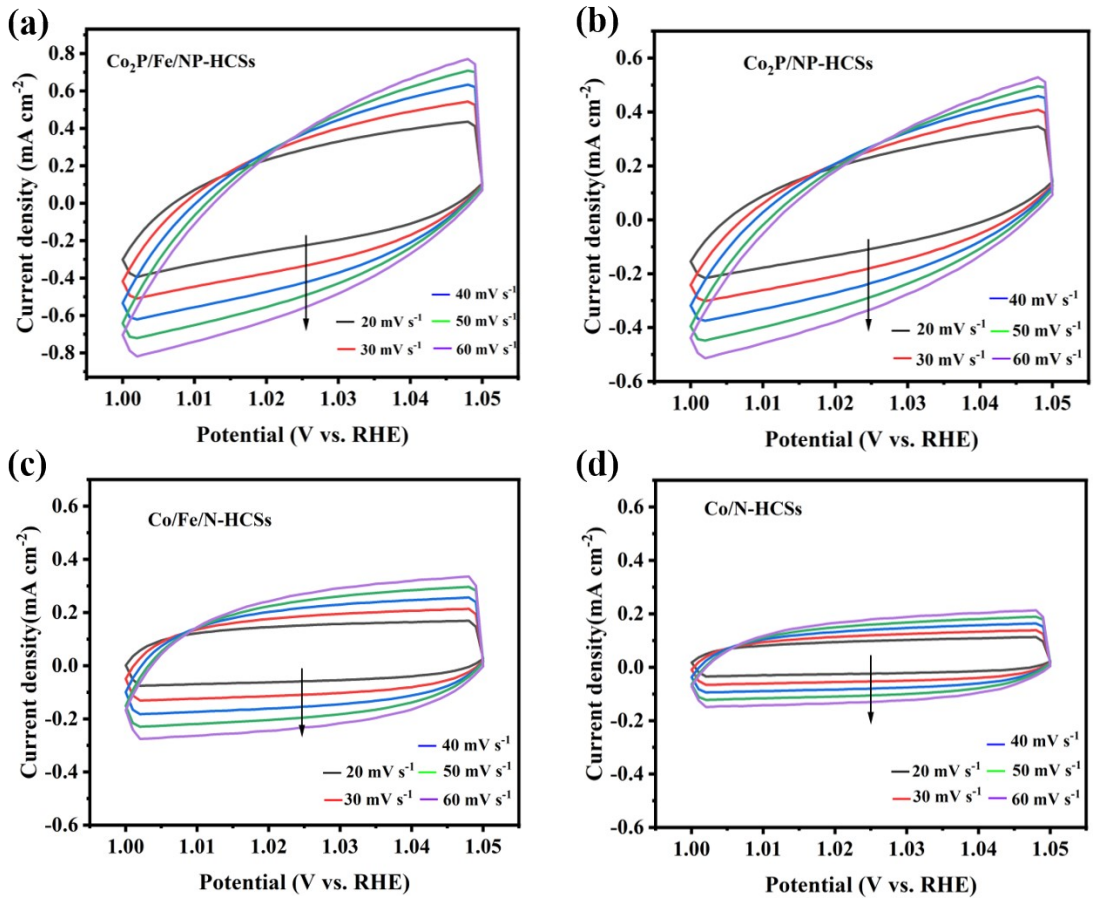

Fig. S10. CV curves of (a) Co_2P/Fe/NP–HCSs, (b) Co_2P/NP–HCSs, (c) Co/Fe/N–HCSs, and (d) Co/N–HCSs at various scan rates in the non-Faradaic region.

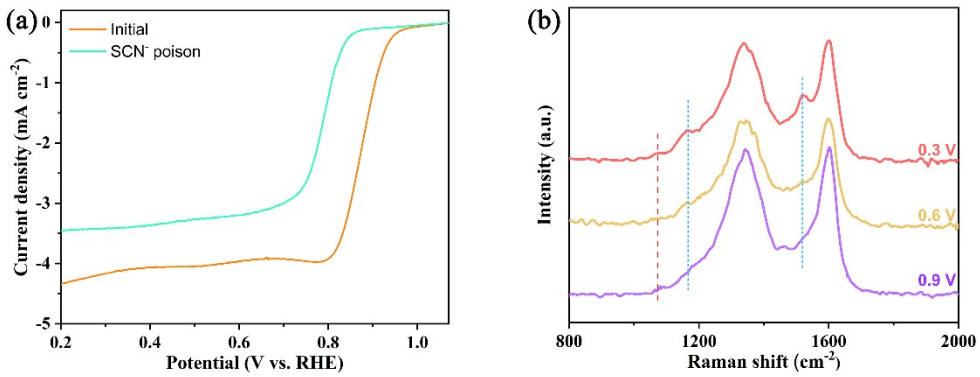

Fig. S11. (a) LSV curves of Co_2P/Fe/NP–HCSs before and after SCN^- poison. (b) *In situ* Raman spectra of Co_2P/Fe/NP–HCSs during the ORR.

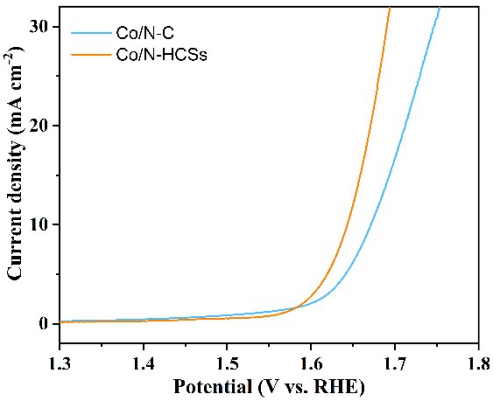

Fig. S12. LSV curves of Co/N-C and Co_2P/Fe/NP–HCSs for OER.

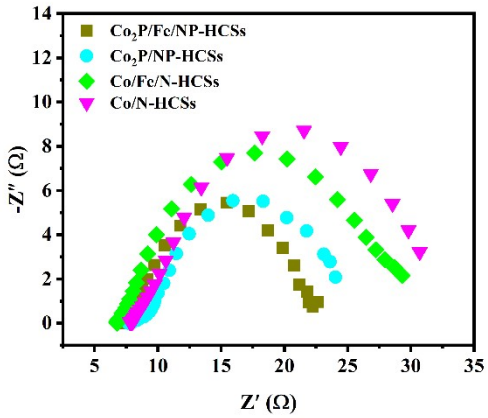

Fig. S13. Nyquist plots of the impedance for different catalysts.

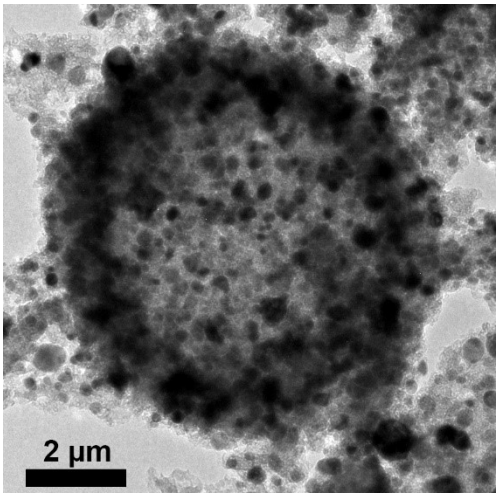

Fig. S14. TEM image of Co_2P/Fe/NP–HCSs after OER test.

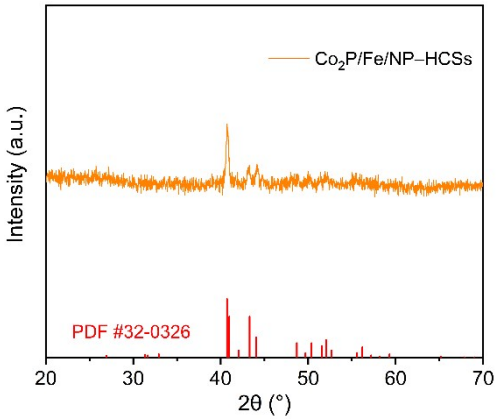

Fig. S15. XRD pattern of Co_2P/Fe/NP–HCSs after OER test.

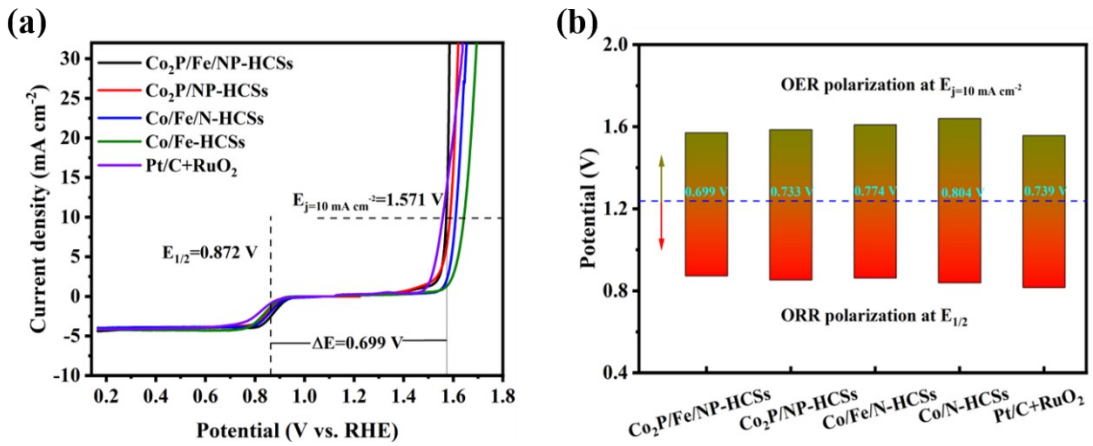

Fig. S16. (a) Bifunctional polarization curves for as-synthesized electrocatalysts in ORR/OER potential range. (b) Diagram to compare the ΔE value of different catalysts.

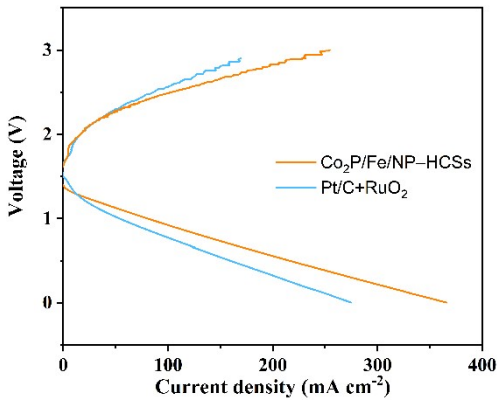

Fig. S17. Charge and discharge curves of the ZAB assembled with Co_2P/Fe/NP–HCSs and Pt/C+RuO_2.

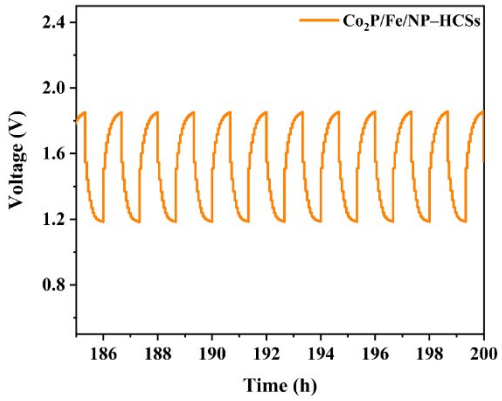

Fig. S18. Charge and discharge polarization curves of ZABs with Co_2P/Fe/NP–HCSs as the air electrode.

Fig. S19. Open circuit voltage of solid-state ZAB tested by a universal meter.

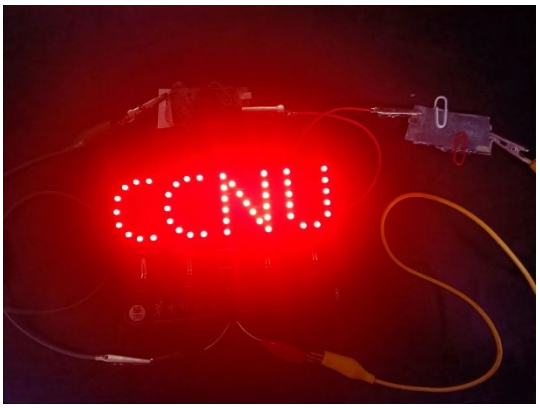

Fig. S20. Photograph of two solid-state ZABs interconnected in series for lighting CCNU bulb.

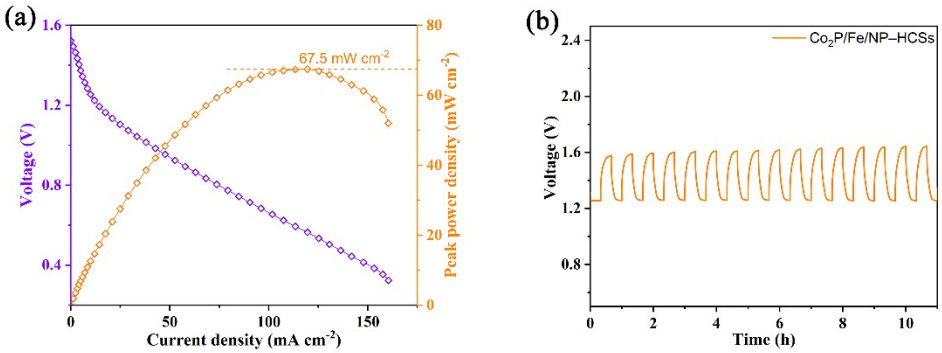

Fig. S21. (a) Discharge polarization curve and peak power density and (b) Charge/discharge cycle of Co_2P/Fe/NP–HCSs-based ZAB at –40 ℃.

Table S1. Comparison of the ORR performance of the Co_2P/Fe/NP–HCSs with other TMPs-based electrocatalysts recently reported.

Catalysts	$E_{1/2}$	$E_{j=10}$	ΔE	Reference
Co_2P/Fe/NP-HCSs	**0.872**	**1.571**	**0.699**	**This work**
FeCo/Co_2P@NPCF	0.790	1.560	0.770	[1]
Co_2P/doped-CNTs-800	0.843	1.603	0.760	[2]
Co_2P@CNF	0.800	1.690	0.890	[3]
CoNiP/PNC	0.840	1.700	0.860	[4]
CoP/NC-800	0.780	1.520	0.740	[5]
Co_2P/CoP@NPC	0.770	1.550	0.780	[6]
Co_2P@CoNPG-900	0.810	1.730	0.920	[7]
Ni,Fe-DSAs/NCs	0.895	1.612	0.717	[8]
Co_4N@d-NCNWs/D	0.83	1.57	0.74	[9]
P-NCO/NCN-CF@CC	0.828	1.588	0.76	[10]
FeN_4-SC-NiN_4	0.844	1.476	0.632	[11]

Reference

[1] Q. Shi, Q. Liu, Y. Ma, Z. Fang, Z. Liang, G. Shao, B. Tang, W. Yang, L. Qin, X. Fang, Adv. Energy Mater. 10 (2020) 1903854.

[2] L. Song, H. Fan, X. Fan, H. Gong, T. Wang, J. He, Chem. Eng. J. 435 (2022) 134612.

[3] J. Gao, J. Wang, L. Zhou, X. Cai, D. Zhan, M. Hou, L. Lai, ACS Appl. Mater. Interfaces 11(10) (2019) 10364-10372.

[4] W. Sun, Y. Xu, P. Yin, Z. Yang, Appl. Surf. Sci. 554 (2021) 149670.

[5] L. Feng, R. Ding, Y. Chen, J. Wang, L. Xu, J. Power Sources 452 (2020) 227837.

[6] Q. Shi, Q. Liu, Y. Zheng, Y. Dong, L. Wang, H. Liu, W. Yang, Energy Environ. Mater. 5(2) (2022) 515-523.

[7] H. Jiang, C. Li, H. Shen, Y. Liu, W. Li, J. Li, Electrochim. Acta 231 (2017) 344-353.

[8] Z Wang, X Jin, R Xu, Z Yang, S Ma, T Yan, C Zhu, J Fang, Y Liu, S-J Hwang, Z Pan, HJ Fan, ACS Nano 17 (2023) 8622.

[9] C Zhang, N Huang, Z Zhai, L Liu, B Chen, B Yang, X Jiang, N Yang, Adv. Energy Mater. 13 (2023) 2301749.

[10] Y Liu, Z Jiang, Z-J Jiang, Adv. Funct. Mater. 33 (2023) 2302883.

[11] K Su, S Yang, A Yang, Y Guo, B Liu, J Zhu, Y Tang, X Qiu, Appl. Catal. B-Environ. 331 (2023) 122694.